Hindawi
Advances in Materials Science and Engineering
Volume 2020, Article ID 6360131, 15 pages
https://doi.org/10.1155/2020/6360131

Research Article

Experimental Study on Rheological Properties and Strength Variation of High Concentration Cemented Unclassified Tailings Backfill

Shijiao Yang, Xing Xing, Shuai Su, and Fulin Wang

School of Resource & Environment and Safety Engineering, University of South China, Hengyang 421001, China

Correspondence should be addressed to Xing Xing; 450775002@qq.com

Received 29 June 2019; Revised 12 December 2019; Accepted 24 December 2019; Published 14 February 2020

Academic Editor: Ilia Ivanov

This experimental study presents the rheological properties and strength characteristics of cemented unclassified tailings backfill (CUTB). The particle size distribution and chemical properties of tailings from the Shizhuyuan lead-zinc mine were examined experimentally. A series of rheological properties and uniaxial compressive strength (UCS) tests were conducted to study the relations between the rheological properties of CUTB and two factors of cement-tailings ratio (c/t) and solid content (SD). The two-factor nonrepetitive analysis of variance (ANOVA) method was used to study the sensitivity of rheological properties to two factors of c/t and SD. Relations between UCS performance of CUTB and c/t, SD, and curing time (CT) were discussed. Results indicate that CUTB samples exhibit obvious shear thinning characteristics and the rheological process is the result of multiple rheological model composites. Yield stress and viscosity of CUTB increase with the increase of SD and c/t as quadratic. The solid content is the most important factor for the rheological properties of CUTB, followed by c/t. UCS of CUTB increases exponentially with the increase of SD and increases with c/t as quadratic. The larger the ratio of c/t, the greater the influence of the CT on the increasing strength of CUTB. The smaller the c/t, the slower the increase of the CUTB's strength with the increase of the SD. The findings of this study can provide the efficient mix proportion of backfill slurry for the backfill mining design, so as to have better performance of the underground mining structure and reduce the cost of backfill mining.

1. Introduction

Mine backfill has gained increasing popularity in the mining industry all over the world due to the fact that it provides ground support for mining operations, reduces ore dilution, and allows safe disposal of tailings [1–3]. Generally, the cemented paste backfill (CPB) is made of complex composite composed of filtered tailings, water, and binders [4] and is transported underground to mine stopes by gravity delivered or pumped through a network of pipelines [5]. The CPB usually uses classified tailings as aggregate leads to a problem of low utilization of tailings. Meanwhile, superfine tailings remaining after classification has always been a treatment and utilization challenges due to safety and environmental problems [6]. Considering the advantages of CPB based on high concentration unclassified tailings, such as realizing the full utilization of tailings, no bleeding, no segregation, and no sedimentation of CPB slurry, this method has become one of the vital development directions of backfill technology. Rheological properties and mechanical properties are two key factors in high concentration unclassified backfill technology, which significantly influence the pipeline transportation of slurry and safety of adjacent stope [7, 8].

The transport pattern of the CPB slurry in the pipeline is different from the traditional two-phase fluid, and it is generally believed to exist in the form of structural flow. It is a common method to calculate the rheological parameters to get the resistance of pipeline by CPB rheology [9]. Numerous studies on the rheological behaviors of backfill slurry have been carried out. Some experimental studies indicated that the slump flow could reflect the rheological properties of

backfill samples intuitively [10, 11]. However, the slump flow cannot reflect the rheological properties from an academic point of view. High concentration slurry is generally considered to be a non-Newtonian fluid. Hence, the viscosity and yield stress are two vitally important parameters, which are often used to evaluate the rheological properties of high concentration slurry [12]. There are many factors that can determine the rheological properties of CPB slurry including external factors [13, 14] (such as temperature and loading pressure) and internal factors (such as solid content and cement content of the CPB mixtures and properties of the CPB mixture constituents) [12, 15–17]. Furthermore, some researchers reported that the time-dependent rheological behavior significantly influences the transportability of CPB slurry due to the fact that the rheological properties of CPB slurry change with time [7, 17, 18].

The uniaxial compressive strength test is most widely used to study the mechanical properties of CPB, which is a simple and economical test method [19]. Numerous previous experimental studies concentrate a lot on the components (tailings, cement, admixture, and water) of CPB mixture which influence the UCS of CPB [2, 4, 19–37]. Megan et al. [38] investigated that curing with elevated temperature and effective stress can significantly increase the UCS of CPB. Yilmaz et al. [8] reported that the stope depth has a positive effect on UCS of CPB, and the UCS of CPB samples near the stope's bottom is always higher than those located at the top of the stope. Qi et al. [39] proposed an intelligent modeling framework for the prediction of CPB's mechanical properties using machine learning algorithms and genetic algorithm. Cao et al. [40–42] and Wang et al. [43, 44] investigated the influence of structural factors (filling time, filling interval time, and filling surface angle) on UCS of CPB.

Although reports about the properties of CPB are numerous, all of them show no quantitative relationship between rheological property parameters and the two factors (solid content (SD) and cement-to-tailings ratio (c/t)), especially for high concentration cemented unclassified tailings backfill (CUTB). This study aims to characterize the rheological property parameters and strength behavior of CUTB using the control variable method. Rheology test on CTUB with different SD and c/t ratios was conducted to reveal the relationship between rheological property parameters and the two factors. The sensitivity of rheological properties to different influencing factors was analyzed by the two-factor nonrepetitive analysis of variance (ANOVA) method. Additionally, the major factors such as the c/t, SD, and curing time (CT) were considered for uniaxial compressive experiments, and relationships between the above three factors and the UCS of CUTB samples were studied. The research results provide a theoretical basis and data reference for an efficient and effective tailings backfill design of such mine.

2. Materials and Experimental Method

2.1. Materials

2.1.1. Tailings. The unclassified tailings used in this study were from Shizhuyuan lead-zinc mine in Hunan province, China. The density and bulk density of the studied tailings are 2550 and 1720 kg/m^3, respectively. The particle size of the tailings was analyzed by S3500 (Microtrac, Florida, USA) laser particle analyzer. The results are shown in Figure 1(a). It was found that the particle composition is $D_{10} = 5.85\,\mu$m, $D_{90} = 362.9\,\mu$m, and $D_{50} = 104.7\,\mu$m, which is a typical coarse-grained tailing. The unevenness coefficient $C_u = 28.051$, and the particle size gradation is good.

The chemical compositions of the tailings were tested by X-ray diffraction, and the results were shown in Figure 1(b) and Table 1. SiO_2 and Fe_2O_3 were the main minerals within the tailings (26.677% and 38.504% by weight).

2.1.2. Binder and Mixing Water. The 32.5R ordinary Portland cement was used as the binding agent during test according to the Chinese No. GB175-2007 and the chemical composition was shown in Table 2. Municipal tap water was used as mixing water to prepare CUTB samples.

2.2. CUTB Samples Preparation. CUTB samples (360 in total) were prepared by blending and homogenizing the lead-zinc unclassified tailings, OPC, and water (Table 3). The mixtures were then casted in metal cubes with dimensions of 70.7 mm × 70.7 mm × 70.7 mm. The CUTB samples were cured in a humidity chamber at 20°C and 95% relative humidity for different curing times (7, 28, and 56 days).

2.3. Rheology Testing. To investigate the rheological properties of the CUTB slurry, the stress and strain of 20 groups of CUTB slurry mixes were tested by MCR52 rheometer (Anton Paar, Graz, Austria), and the rotor was measured with ST24-2D/2V-30 paddle rotor (diameter/height: 20/40 mm). The operating software was RheoCompass rheometer software. The experiment adopts the controlled shear rate (CSR) mode for parameter design. Compared with the test method for controlling the shear stress (CSS), the range of the slurry rheological characteristic curve of the CCR method is more comprehensive, and the rheological properties of the whole process of the slurry transition from the low-speed state to the high-speed state can be reflected. The measurement parameters are set to non-Newtonian fluid mode. The prepared CUTB slurry was poured into a cylindrical glass beaker (D/H: 95/122 mm) and bubbles were removed in the mix. The CUTB samples were tamped. The shear time was set to 120s, and the shear rate increased linearly from 0 to 10^2s^{-1}. The temperature was 20°C at room temperature to avoid the effects of temperature changes. The software automatically may save the yield stress and fluid viscosity data, and the operating software can automatically generate the rheological curve after each experimental test is completed. The RheoCompass rheometer software can form a corresponding linear fitting curve to monitor the output shear stress-shear rate curve and viscosity-shear rate curve in real time.

2.4. Uniaxial Compressive Testing. UCS tests of CUTB samples were performed using an electrohydraulic pressure

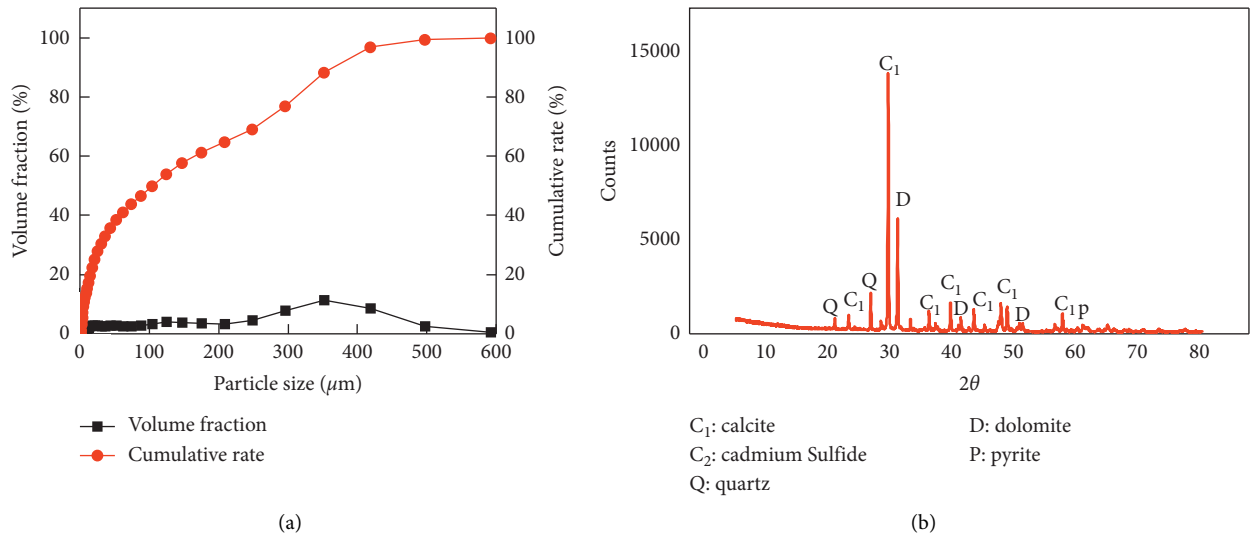

Figure 1: Fundamental characteristics of the studied tailings: (a) particle size distribution curve; (b) X-ray diffraction curve.

Table 1: Chemical composition of the tailings used.

Varieties (%)	SiO_2	Al_2O_3	MgO	Fe_2O_3	CaO	MnO	Na_2O	ZnO	TiO_2	PbO	K_2O	Loss
Tailings	26.677	4.529	1.502	38.504	10.961	1.04	2.413	6.253	0.328	0.664	1.979	5.15

Table 2: Chemical composition of the binder used.

Varieties (%)	CaO	SiO_2	Al_2O_3	Fe_2O_3	SO_3	MgO
OPC 32.5R	61.42	22.21	5.18	3.28	2.46	2.49

Table 3: Mix formulations of cemented unclassified tailings backfill mixture.

Cement-to-tailings ratio (c/t)	Solid content (%)
1 : 04	72
1 : 08	74
1 : 12	76
1 : 16	78
	80

testing machine (Xinluda, Wuxi, China) with a 300 WR loading capacity for uniaxial compression chamber test; the loading rate was set to 0.5 mm/min according to ASTM C39 [45].

3. Results and Discussion

3.1. Rheological Properties Parameter Results of CUTB Samples. Carrying out research on the rheological properties of the unclassified tailings slurry to obtain rheological data (such as viscosity and yield stress) can provide good theoretical support for the fluidity of the slurry, the ease of pipeline transportation, and the design of the transportation pipeline. At the same time, the mix proportion range that meets the needs of engineering is obtained by rheological test, which also provides a reference for the compressive strength test.

The yield stress is the adhesion and friction between the particles in the slurry. When the shear stress acting on the slurry is higher than the yield stress, the slurry begins to flow [46]. The yield stress can be tested directly by rheometer and calculated by the maximum torque measured by the rheometer and the size of the mixing blade. The calculation formula was listed in equation (1), and calculation results were listed in Table 4.

$$\tau = \frac{M_0}{[(h/d + 1/3) \times (\pi d^3/2)]}, \quad (1)$$

where τ is the yield stress of the CUTB slurry, M_0 is the maximum torque of blade, h is the height of the mixing blade, and d is the diameter of the mixing blade.

Considering that the slurry is always in the dynamic process during the rheological test, apparent viscosity at the moment cannot effectively and comprehensively reflect the rheological properties of CUTB slurry. Therefore, the arithmetic means of viscosity throughout the shear time were used to reflect the rheological property of CUTB slurry and calculation was listed in equation (2). The corresponding calculation results were listed in Table 4.

$$\eta = \frac{\eta_1 + \eta_2 + \cdots + \eta_n}{n}, \quad (2)$$

where η is the viscosity of CUTB slurry and n is the number of test records.

Table 4 shows the mean viscosity and yield stress results of CUTB with different SD and c/t ratio values. Results indicate that, for a c/t ratio of 1 : 04, mean viscosity significantly increases from 5.56 Pa·s to 80.83 Pa·s and yield stress increases from 34.13 Pa to 545.19 Pa when the CUTB's

Table 4: Rheological parameters results of CUTB samples.

Cement-to-tailings ratio (c/t)	Solid content (%)	Viscosity (Pa·s)	Yield stress (Pa)
1 : 04	72	5.56	34.13
	74	6.75	45.03
	76	16.37	103.63
	78	48.92	337.73
	80	80.83	545.19
1 : 08	72	4.08	26.79
	74	6.59	43.02
	76	11.88	77.59
	78	35.62	224.92
	80	56.49	388.85
1 : 12	72	3.42	23.64
	74	5.97	39.81
	76	11.44	72.62
	78	26.09	170
	80	55.32	375.65
1 : 16	72	3.35	23.48
	74	5.47	36.26
	76	10.52	69.45
	78	22.14	141.96
	80	54.52	370.09

SD increases from 72% to 80%. Nevertheless, when the cement-to-tailings ratio for CUTB slurry increases from 1 : 04 to 1 : 16, the corresponding mean viscosity decreases from 5.56 Pa·s to 3.35 Pa·s and yield stress of CUTB slurry decreases from 34.13 Pa to 23.48 Pa for a fixed solid content of 72 wt.%.

3.1.1. Analysis of Apparent Viscosity. Apparent viscosity is calculated as shear stress divided by the corresponding shear rate [47], and the apparent viscosity reflects the degree of shear stress at a given shear rate. The apparent viscosity of the Newtonian material is independent of the shear rate. For Bingham or pseudoplastic materials, the apparent viscosity is usually not a fixed value but decreases as the shear rate increases. The apparent viscosity and shear rate curve were obtained automatically by RheoCompass software. Part of the results is shown in Figure 2 due to the limited space.

It is evident from Figure 2(a) that the apparent viscosity of the slurry is positively correlated with the solid content. The variation of CUTB slurry's apparent viscosity is not obvious at the low SDs (72–76 wt.%), but it is significantly increased at the high SDs (78–80 wt.%).

In addition, when the value of solid contents is lower than 78 wt.%, the variation of the CUTB slurry's apparent viscosity with shear rate can be divided into three phases. The first phase is a rapid decrease in apparent viscosity (0–10 s^{-1}). The initial apparent viscosity of the CUTB slurry is very large, and it is necessary to destroy the internal floc structure to make the slurry flow. At this phase, the apparent viscosity drops sharply, and the flow capacity increases rapidly. The second phase is a linear decrease in apparent viscosity (10–60 S^{-1}). During this phase, as the shear rate increases, the CUTB slurry's apparent viscosity decreases slowly and tends to be in a dynamic stability state. At last, the dynamic stability of apparent viscosity is the third phase, which exhibits shear thinning behavior. An explanation for this behavior is that the fine particles inside the slurry are continuously dispersed, collided, aggregated, and redispersed under the action of higher shear rate [18], and the slurry behaves as Newtonian. Furthermore, the similar characteristics of CUTB slurry at different c/t ratio also can be seen from Figure 2(b).

When the value of solid contents is higher than 78 wt.%, the variation of the apparent viscosity of CUTB slurry with increased shear rate can be divided into two stages: rapid reduction (0–20 s^{-1}) and gradual decrease (20 s^{-1}). This variation showed a noticeable derivative trend, and with the shear rate increasing, the slurry behaves as Bingham or similar Bingham after a short shear.

It can be noticed from Figure 2(b) that the CUTB slurry's apparent viscosity changed as a derivative function at different c/t ratio. This behavior indicates that the c/t ratio has little effect on the apparent viscosity of the slurry and controlling appropriate solid content of CUTB slurry is the key in pipeline transportation.

3.1.2. Analysis of Yield Stress. The two-factor nonrepetitive analysis of variance was used to study the influence degree of c/t ratio and solid content on the yield stress of CUTB slurry, and the ANOVA data and analyzed results were listed in Tables 5 and 6, respectively. Given the value of significant level (α) of 0.05, check the critical value F checklist to get $F_{0.05}$ (3, 12) = 3.49 and $F_{0.05}$ (4, 12) = 3.26.

It can be seen from Table 6 that the value of F_x (3.974) is larger than $F_{0.05}$ (3, 12) = 3.49 and F_Y = 58.758 is larger than $F_{0.05}$ (4, 12) = 3.26, which indicate that factor X (cement-to-tailings ratio) and factor Y (solid content) both significantly influence the yield stress of CUTB slurry. Additionally, the influence of c/t ratio is significantly larger than the influence

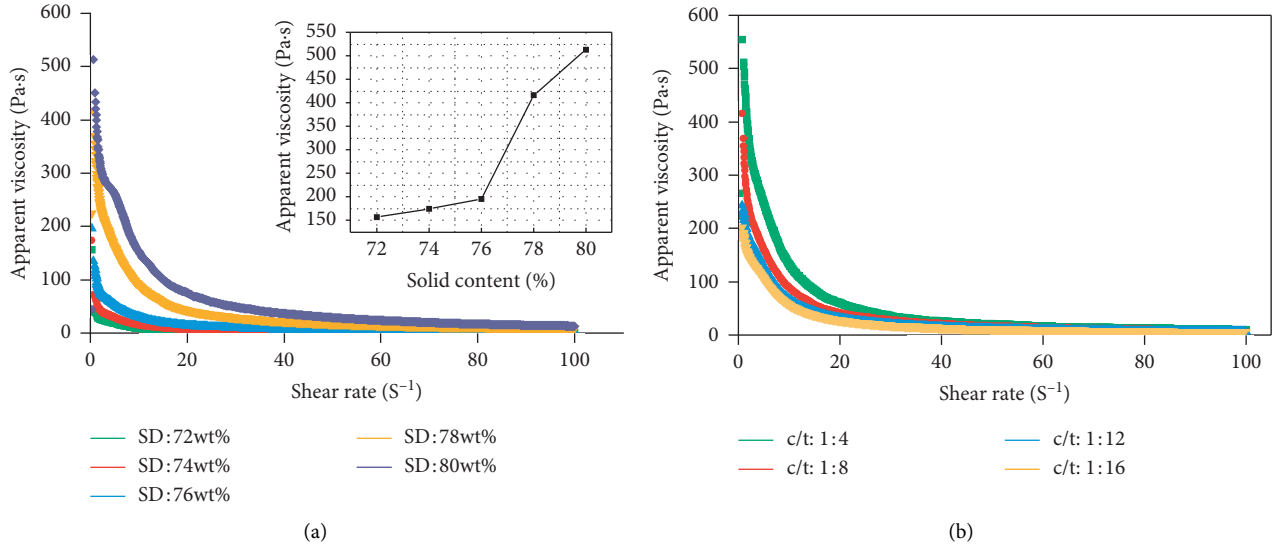

Figure 2: Relationship between apparent viscosity and shear rate with different c/t ratio and SD: (a) c/t ratio of 1 : 08; (b) SD of 78%.

Table 5: ANOVA data of CUTB samples.

Solid content (%)	Yield stress (Pa)			
	(X_1) c/t: 1 : 04	(X_2) c/t: 1 : 08	(X_3) c/t: 1 : 12	(X_4) c/t: 1 : 16
(Y_1) 72	34.13	26.79	23.64	23.48
(Y_2) 74	45.03	43.02	39.81	36.26
(Y_3) 76	103.63	77.59	72.62	69.45
(Y_4) 78	337.73	224.92	170	141.96
(Y_5) 80	545.19	388.85	375.65	370.09

Table 6: ANOVA results of CUTB samples.

Source of variance	Sum of squares	Degree of freedom	Mean square error	Value of F	F_α (n_1,n_2)	Significant level
X	22135.093	3	7378.364	3.974	$F_{0.05}$ (3, 12) = 3.49	0.035
Y	436357.384	4	109089.346	58.758	$F_{0.05}$ (4, 12) = 3.26	0.000
Error	22279.230	12	1856.603			
Total	480771.707	19				

of SD on the yield stress of CUTB slurry according to the comparison of the differential values between F (F_X and F_Y) and $F_{0.05}$.

The CUTB slurry based on unclassified tailings contains a certain number of particles with a smaller particle size which forms a skeleton structure as to resist shearing when the slurry is static. This structure will make the slurry have a certain cohesion, and the yield stress is the force that enables the slurry to begin to flow as the torque increases. Figure 3 represents the fitted histogram of solid content and yield stress of CUTB slurry. One can say that the value of the increase in yield stress significantly increases with the solid content increasing from 72% to 80%. Setting the cement-to-tailing ratio of 1 : 08 as an example, the value of yield stress increases from 26.79 Pa to 43.02 Pa when the solid content increased from 72% to 74%, and the values of increase were not obvious. When the solid content increased from 74% to 80% respectively, the corresponding slurry yield stress with a

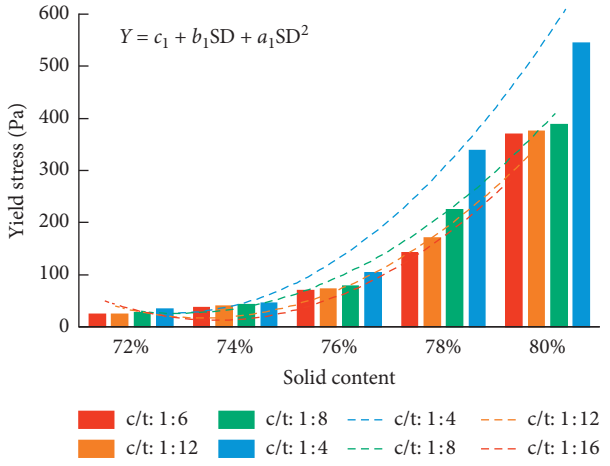

Figure 3: Histogram between SD and yield stress of CUTB samples.

Table 7: Yield stress fitting results of CUTB samples under various SDs.

Cement-to-tailings (c/t)	Correlation coefficient (R^2)	c_1	b_1	a_1
1 : 04	0.989	53784.686	−1477.656	10.154
1 : 08	0.995	38749.838	−1062.562	7.289
1 : 12	0.990	42649.936	−1162.157	7.920
1 : 16	0.976	45504.412	−1235.823	8.393

c/t ratio of 1 : 08 increased from 43.02 Pa to 77.59 Pa, 224.92 Pa, and 388.85 Pa. The values of the increase in yield stress were approximately 35 Pa, 182 Pa, and 346 Pa, which became more and more big. In addition, the variations of the yield stress of CUTB slurry with c/t ratios of 1 : 04, 1 : 12, and 1 : 16 are similar to the CUTB's c/t ratio of 1 : 08. The reason behind this increase is that the yield stress is the resistance that needs to be overcome during the initial flow of the slurry. This resistance is caused by the adhesion and friction between the particles inside the slurry. When the interdependence and frictional effects between the particles increase or decrease, the yield stress will increase or decrease. The high-quality concentration of the slurry is due to the high solid content, the free water content of the lubrication is relatively low, resulting in increased flow resistance, and the yield stress of the mixture is also increasing.

The cement-to-tailings ratio was considered as constant to better investigate the relationship between the yield stress of CUTB slurry and different solid content. Quadratic fitting of the variation of yield stress was conducted and the relevant correlation coefficient (R^2) and equation parameters were listed in Table 7.

It was found from Table 7 that quadratic fitting methods have great regression degrees. The average value of multiple R^2 is greater than 0.97, which shows that the relationship between solid content and yield stress of CUTB slurry could be well expressed as the quadratic equation, and the relevant expression can be defined as

$$Y = c_1 + b_1 \times \mathrm{SD} + a_1 \times \mathrm{SD}^2, \tag{3}$$

where Y is the yield stress of the CUTB slurry, SD is the solid content, and c_1, b_1, and a_1 are the fitting parameters related to the influence of solid content and yield stress factors.

Figure 4 shows the fitted histogram curves between cement-to-tailings ratio and yield stress of CUTB slurry. One can say from the results that, for a given SD in the mix, the yield stress of CUTB slurry increases as the c/t ratio of CUTB slurry increases. Among them, when the SD of the slurry was lower than 78 wt.%, the increased range of yield stress of CUTB slurry was not obvious. For CUTB slurry with solid content higher than 78 wt.%, the increased range of yield stress of CUTB slurry had a significant increase.

To better investigate the relationship between yield stress values and cement-to-tailings ratio for CUTB slurry, the solid content was fixed. Quadratic fitting of the variation of yield stress was conducted and the relevant correlation coefficient (R^2) and equation parameters were listed in Table 8.

It was found from Table 8 that quadratic fitting methods have great regression degrees. The corresponding average

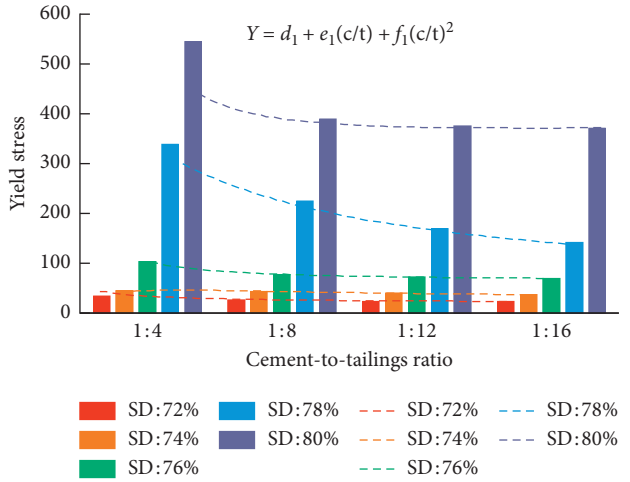

Figure 4: Histogram between c/t and yield stress of CUTB samples.

value of multiple R^2 is larger than 0.98, which shows that the relationship between c/t ratio and yield stress of CUTB slurry could be well expressed as the quadratic equation. The relevant expression can be definedas

$$Y = e_1 + d_1\,(\mathrm{c/t}) + f_1\,(\mathrm{c/t})^2, \tag{4}$$

where Y is the yield stress of the CUTB slurry and c/t is the cement-to-tailings ratio. d_1, e_1, and f_1 are the fitting parameters related to the influence of cement-to-tailings ratio and yield stress factors.

3.1.3. Analysis of Mean Viscosity. The two-factor nonrepetitive analysis of variance (ANOVA) was used to study the influence degree of c/t ratio and solid content on the viscosity of CUTB slurry, and the analyzed results were listed in Table 9. Given the value of significant level (α) of 0.05, check the critical value F checklist to get $F_{0.05}$ (3, 12) = 3.49 and $F_{0.05}$ (4, 12) = 3.26.

Table 10 shows that F_x (4.134) and F_Y (61.429) are both larger than corresponding critical value F_α. Therefore, the two factors have a significant influence on the mean viscosity of CUTB slurry. Additionally, the influence of SD is significantly larger than the influence of c/t ratio on the viscosity of CUTB slurry according to the comparison of the differential values between F (F_X and F_Y) and $F_{0.05}$.

Figure 5 shows the histogram curves between cement-to-tailings ratio and the mean viscosity of CUTB slurry. One can say that mean viscosities of the CUTB slurry with low solid contents (72–76 wt.%) have lower values (3.35–16.37 Pa·s). As expected, the higher the solid contents

Table 8: Yield stress fitting results of CUTB samples under various c/t ratios.

Solid content (%)	Correlation coefficient (R^2)	d_1	e_1	f_1
72	0.993	20.008	47.751	35.306
74	0.989	26.048	199.714	−495.475
76	0.999	64.925	51.665	412.306
78	1.000	40.622	1753.164	−2258.335
80	1.000	392.570	−652.635	5051.039

Table 9: ANOVA data of CUTB samples.

Solid content (%)	Viscosity (Pa)			
	(X_1) c/t: 1 : 04	(X_2) c/t: 1 : 08	(X_3) c/t: 1 : 12	(X_4) c/t: 1 : 16
(Y_1) 72	5.56	4.08	3.42	3.35
(Y_2) 74	6.75	6.59	5.97	5.47
(Y_3) 76	16.37	11.88	11.44	10.52
(Y_4) 78	48.92	35.62	26.09	22.14
(Y_5) 80	80.83	56.49	55.32	54.52

Table 10: ANOVA results of CUTB samples.

Source of variance	Sum of squares	Degree of freedom	Mean square error	Value of F	F_α (n_1, n_2)	Significant level
X	475.601	3	158.534	4.134	$F_{0.05}$ (3, 12) = 3.49	0.032
Y	9422.481	4	2355.620	61.429	$F_{0.05}$ (4, 12) = 3.26	0.000
Error	460.166	12	38.347			
Total	10358.248	19				

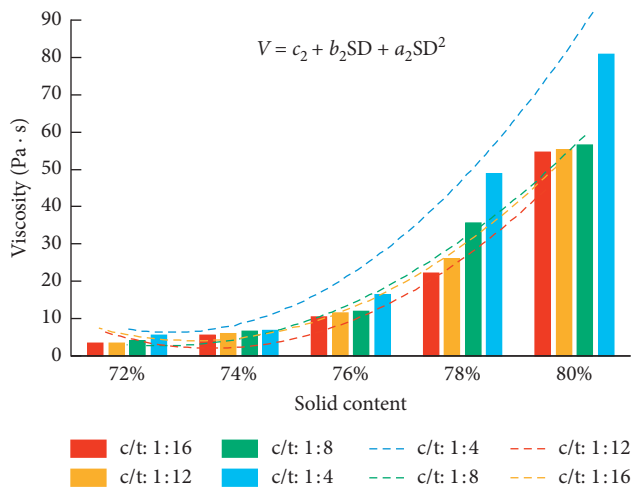

Figure 5: Histogram between SD and viscosity of CUTB samples.

(78–80 wt.%) yield, the higher the mean viscosities (22.14–80.83 Pa·s). This is mainly due to the fact that the higher solid content means a higher aggregate content, which increases the probability of collision between fine particles of CUTB while also increasing the internal friction of CUTB. Additionally, when the solid contents are lower than 76%, the mean viscosity does not change significantly as the solid content increases. However, the mean viscosity of CUTB increases obviously when the solid contents are higher than 76%, which is 2–3 times the CUTB with solid content of 76%. With the solid contents of 80%, the variation of mean viscosity does not conform to the overall variation law.

The cement-to-tailings ratio was considered as constant to better study the variation of the viscosity of CUTB slurry with different solid content. Quadratic fitting of the variation of mean viscosity was conducted and the relevant correlation coefficient (R^2) and equation parameters were listed in Table 11.

It was found from Table 11 that the quadratic fitting methods have great fitting degrees. The corresponding multiple R^2 are larger than 0.98, which shows that the relationship between solid content and slurry viscosity could be well expressed as the quadratic equation, and the relevant expression can be defined as

$$V = c_2 + b_2SD + a_2SD^2, \quad (5)$$

where V is the viscosity of the CUTB slurry, SD is the solid content, and c_2, b_2, and a_2 are the fitting parameters related to the influence of solid content and viscosity factors.

It is evident from Figure 6 that as the solid content of CUTB slurry increases from 72 wt.% to 80 wt.%, the mean viscosity of the slurry with a c/t ratio of 1 : 04, 1 : 08, 1 : 12, and 1 : 16 increases from 5.56 to 80.83 Pa·s, from 4.08 to 56.49 Pa·s, from 3.42 to 55.32 Pa·s, and from 3.35 to 54.52 Pa·s, respectively. This behavior can be explained by the viscosity as an apparent characteristic of the internal structure of the slurry, which may hinder the flow performance. Its size depends mainly on the amount of flocculation structure inside the slurry and the degree of damage. The high hydration of the slurry to produce more hydrated

Table 11: Viscosity fitting results of CUTB samples under various SDs.

Cement-to-tailings (c/t)	Correlation coefficient (R^2)	c_2	b_2	a_2
1 : 04	0.993	7989.498	−219.369	1.507
1 : 08	0.989	5196.812	−143.055	0.985
1 : 12	0.993	5991.172	−163.555	1.117
1 : 16	0.981	6477.232	−176.151	1.198

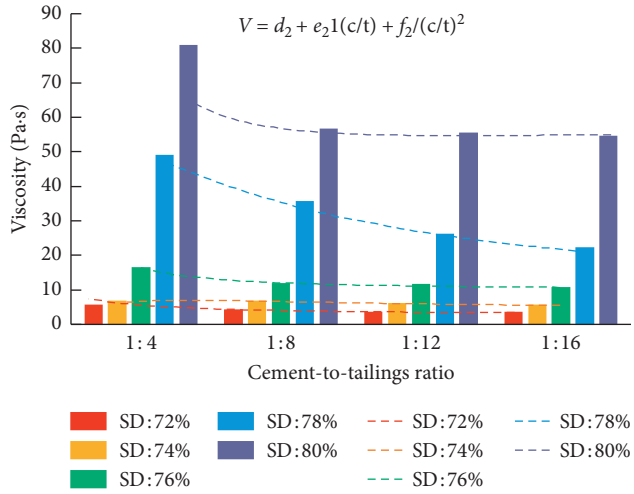

Figure 6: Histogram between c/t and viscosity of CUTB samples.

products will increase the internality of the slurry. Additionally, the adhesion between the particles forms a flocculated structure and a network structure, thereby hindering the flow of the particles and increasing the viscosity of the slurry.

The solid content was considered as constant to better study the variation of the viscosity of CUTB slurry with different cement-to-tailings ratio. Quadratic fitting of the variation of viscosity was conducted and the relevant correlation coefficient (R^2) and equation parameters were listed in Table 12.

Table 12 shows that the quadratic fitting methods have great regression degrees. The corresponding multiple R^2 are larger than 0.98, which shows that the relationship between cement-to-tailings ratio and slurry viscosity could be well expressed as the quadratic equation, and the relevant expression can be defined as

$$V = d_2 + e_2\,(\mathrm{c/t}) + f_2\,(\mathrm{c/t})^2, \tag{6}$$

where V is the viscosity of the CUTB slurry mixes, SD is the solid content, and d_2, e_2, and f_2 are the fitting parameters related to the influence of cement-to-tailings ratio and viscosity factors.

3.2. Analysis of the Variation Law of Backfill's Compressive Strength. The solid content, cement-to-tailings ratio, and curing time are the three main factors affecting the strength of CUTB. In this study, single-factor nonlinear regression analysis was performed on the experimental results using the SPSS Statistics software (IBM, Armonk, USA) to evaluate the quantitative relationship between the CUTB's strength and the three factors.

The regression models were obtained by using SPSS software according to the comparison between the value of the complex correlation coefficient (R^2) and test coefficient index (F) of different regression models.

3.2.1. Uniaxial Compressive Strength Results of CUTB Samples. A total of 360 CUTB samples were prepared and conducted to UCS testing for this study. Each group was tested 6 times, and the average results were obtained for comparison. The UCS values obtained from the testing were shown in Table 13.

One can note from Table 13 that the CUTB strength increases remarkably when the c/t ratio increases from 1 : 04 to 1 : 16, regardless of solid content and curing time. The c/t ratio is the main factor affecting the compressive strength of the CUTB. With the increase of curing time, the cement can produce a large number of hydration products such as C-S-H and ettringite with strong gelling properties during the hydration reaction and the internal compactness increases the strength of the CUTB. In addition, the strength of the CUTB increases as the solid content increases. This behavior can be explained by the fact that the solid content of the slurry is essentially the amount of water content, and a part of the water in the slurry acts as adsorption to connect the particles in the slurry into a net and another part plays a hydration role to form the strength of the CUTB. From the microscopic point of view, the formation of voids in the CUTB is mainly due to the action of water, while the voids in

Table 12: Viscosity fitting results of CUTB samples under various c/t ratios.

Solid content, SD (wt.%)	Correlation coefficient (R^2)	d_2	e_2	f_2
72	0.994	2.551	11.624	1.716
74	0.998	3.679	34.530	−88.999
76	0.991	9.984	7.279	72.849
78	0.998	3.649	325.587	−577.606
80	0.999	59.746	−132.221	865.893

Table 13: The uniaxial compressive strength test results of different CUTB samples.

Cement-to-tailings ratio	Solid content (%)	Curing time (days)		
		7 days (MPa)	28 days (MPa)	56 days (MPa)
1 : 04	72	2.13	2.84	3.11
	74	2.45	3.58	3.97
	76	2.86	4.26	4.52
	78	3.84	6.58	6.83
	80	4.32	7.11	7.34
1 : 08	72	0.51	0.83	0.97
	74	0.67	0.98	1.24
	76	0.84	1.37	1.62
	78	1.17	1.93	2.15
	80	1.29	2.27	2.72
1 : 12	72	0.23	0.38	0.54
	74	0.27	0.51	0.67
	76	0.51	0.77	0.92
	78	0.64	1.06	1.31
	80	1.15	1.71	1.93
1 : 16	72	0.21	0.25	0.31
	74	0.28	0.35	0.42
	76	0.46	0.52	0.56
	78	0.58	0.73	0.82
	80	0.81	0.93	1.05

the CUTB significantly weaken the compressive strength. Controlling the applicable solid content of CUTB is of great importance in improving the safety of pipeline transportation while satisfying the requirements of strength. Therefore, it is especially important to study the relationship between the solid content and the CUTB's strength.

3.2.2. Effect of Solid Content. Histograms and exponential fitting curves of the CUTB strength of different solid content and curing time are shown in Figure 7. As expected, the compressive strength of CUTB samples increases with increasing SD for a given c/t ratio. For an SD of 72 wt.% at a constant c/t ratio of 1 : 04, the strength of 7-day cured CUTBs is 2.13 MPa. When the SD increased from 72 wt.% to 80 wt.%, the corresponding UCS became 4.32 MPa, causing a 50.7% increase in the strength of CUTB. As the SD is increased from 72 wt.% to 80 wt.%, UCS increases from 2.84 to 6.58 MPa for 28 days and from 3.11 to 6.83 MPa for 56 days, respectively. Under the condition of high solid content, the strength of the CUTB samples increases exponentially with the increase of solid content. The smaller the cement-to-tailing ratio is, the slower the backfill's strength increases with the solid content. When the cement-to-tailings ratio is less than or equal to 1 : 08, the backfill's strength increases slowly with the increase of solid content.

The cement-to-tailings ratio and curing time values were considered as constants to study the variation of the CUTB strength in five levels of solid content (72%, 74%, 76%, 78%, and 80%). Exponential fitting of the variation of mixture viscosity was conducted and the relevant correlation coefficients (R^2) were listed in Table 14.

Table 14 shows that an obviously exponential relationship exists between CUTB's solid content and UCS of CUTB. The corresponding multiple correlation coefficients (R^2) for the exponential fit were 0.968, 0.988, 0.978, and 0.994, respectively. The relationship between the SD and UCS of the CUTB samples can be expressed as an exponential equation, and the relevant expression can be defined as

$$\mathrm{UCS} = e^{A_1 + \left(B_1/\mathrm{SD}\right)}, \tag{7}$$

where UCS is the uniaxial compressive strength of the CUTB samples and SD is the solid content. A_1 and B_1 are the fitting parameters related to the influence of solid content and UCS factors. These fitting parameters were listed in Table 15.

3.2.3. Effect of Cement-to-Tailings Ratio. Figure 8 represents the quadratic fitted scatter plot of strength gain of CUTB samples versus c/t ratio with different curing time and solid content. One can observe from the performed test results

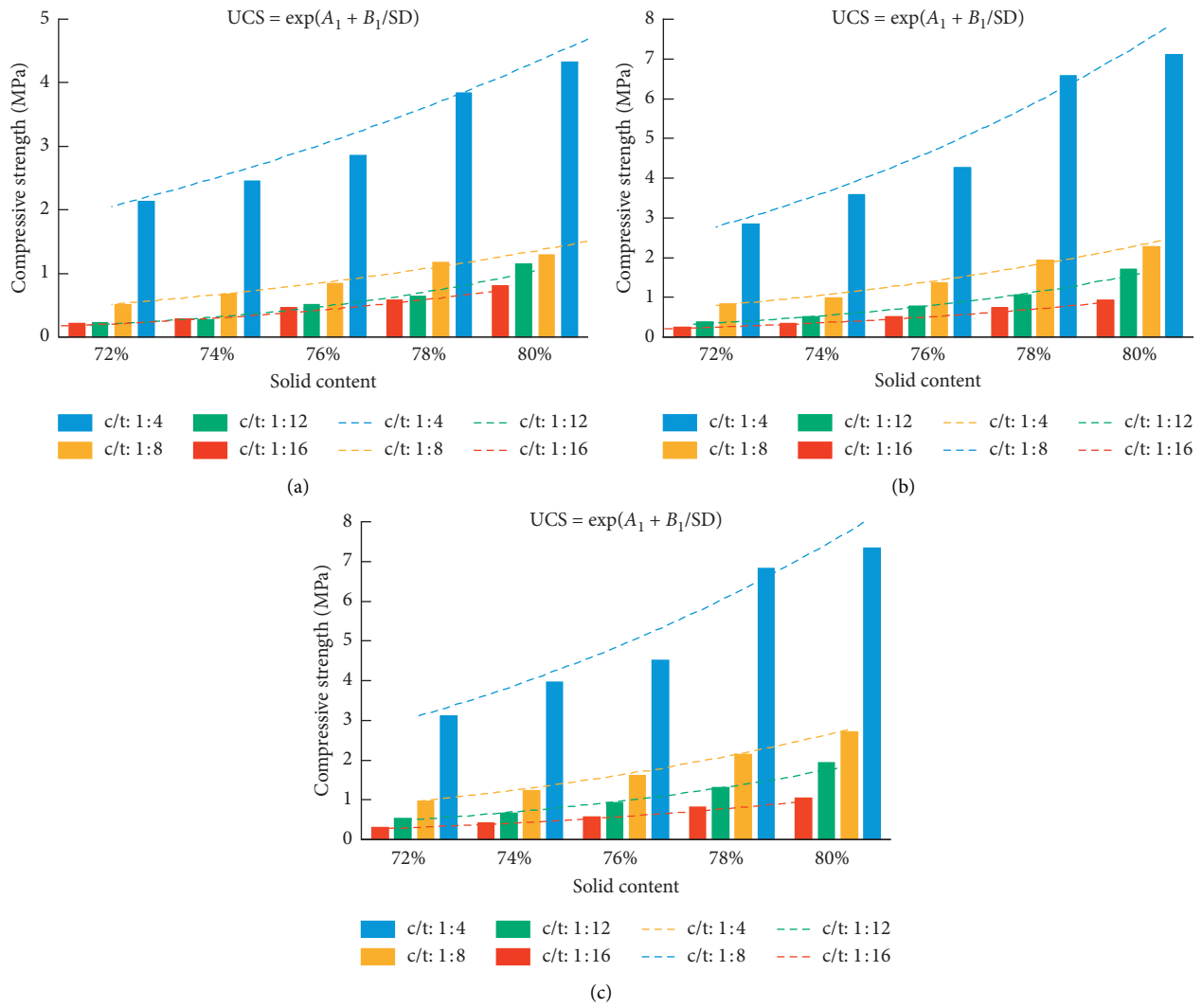

Figure 7: Relationship between SD and UCS of CUTB: (a) CT : 7 d; (b) CT : 28 d; (c) CT : 56 d.

Table 14: UCS results of CUTB samples under various SDs.

Cement-to-tailings ratio (c/t)	Curing time (days)			
	7 days	28 days	56 days	Average
1 : 04	0.976	0.965	0.962	0.968
1 : 08	0.985	0.982	0.998	0.988
1 : 12	0.962	0.989	0.983	0.978
1 : 16	0.990	0.997	0.996	0.994

Table 15: Equation parameters results under various SDs.

Curing time (d)	Cement-to-tailings ratio (c/t)	A_1	B_1
7	1 : 04	8.160	−5.357
	1 : 08	9.010	−6.965
	1 : 12	14.685	−11.716
	1 : 16	12.145	−9.880
28	1 : 04	10.796	−7.038
	1 : 08	10.518	−7.742
	1 : 12	13.895	−10.744
	1 : 16	12.081	−9.697
56	1 : 04	10.164	−6.509
	1 : 08	10.395	−7.520
	1 : 12	12.132	−9.233
	1 : 16	11.239	−8.950

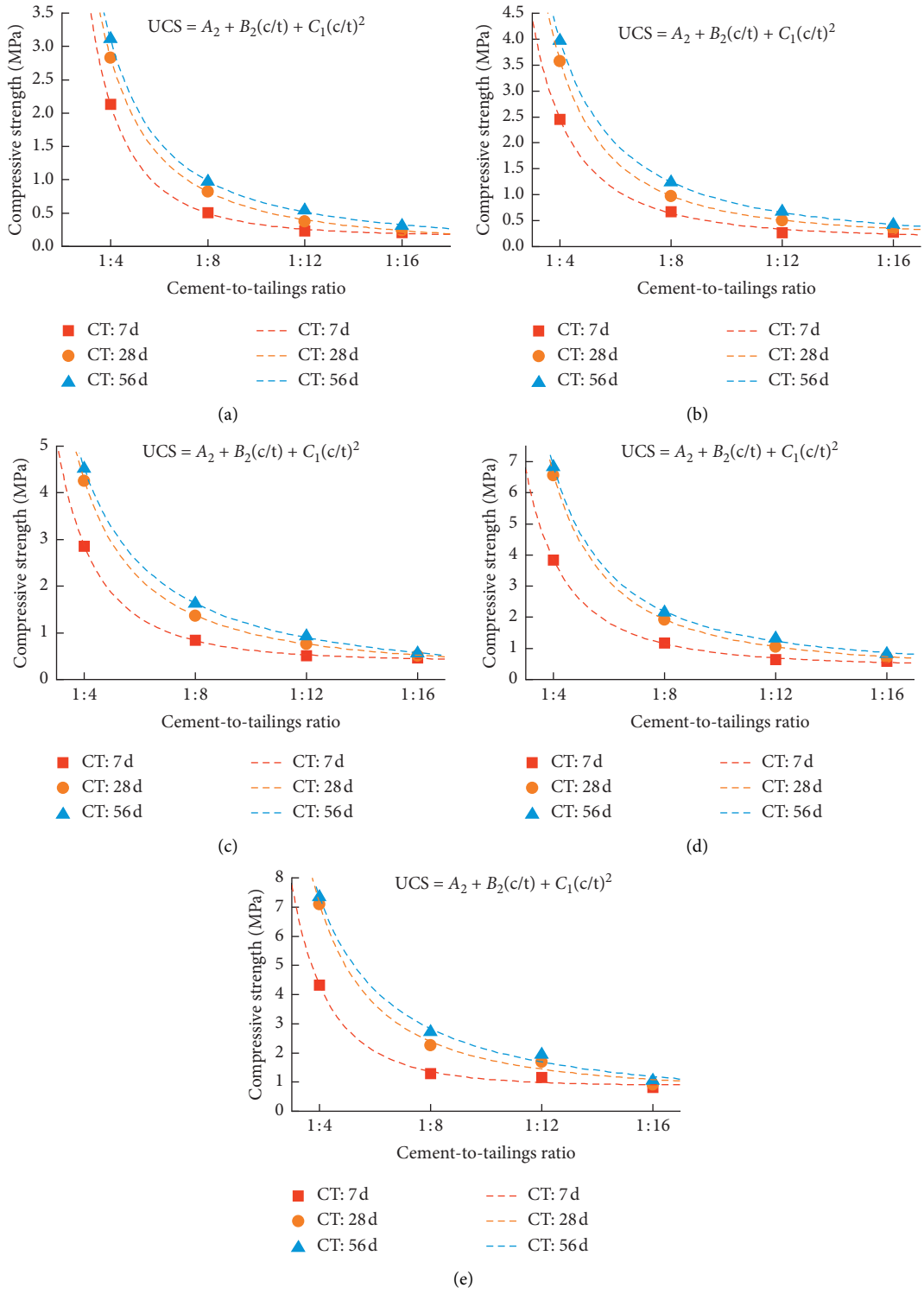

Figure 8: Relationship between c/t and UCS of CUTB: (a) SD : 72%; (b) SD : 74%; (c) SD : 76%; (d) SD : 78%; (e) SD : 80%.

that, for a given solid content in the mix, the mechanical strength gain of CUTB samples increases with an increase in the cement-to-tailings ratio, irrespective of curing time. Under different solid content, the compressive strength of the CUTB with a cement-to-tailings ratio of 1 : 16 hardly increased with the increase of curing time. When the cement-to-tailings ratio increased from 1 : 16 to 1 : 04, respectively, the corresponding compressive strength of CUTB samples with a solid content of 76 wt.% increased from 0.46 to 2.86 MPa for 7 days, from 0.52 to 4.26 MPa for 28 days,

Table 16: UCS results of CUTB samples under various c/t ratios.

Solid content (%)	Curing time (days)			
	7 days	28 days	56 days	Average
72	0.999	0.999	0.999	0.999
74	0.998	0.999	0.999	0.999
76	0.999	0.999	0.999	0.999
78	0.999	0.999	0.999	0.999
80	0.995	0.996	0.996	0.996

Table 17: Equation parameters results under various c/t ratios.

Solid content (%)	Curing time (d)	A_2	B_2	C_1
72	7	0.232	−3.336	43.735
72	28	−0.061	2.498	36.429
72	56	−0.059	3.977	34.781
74	7	0.178	−1.701	43.191
74	28	0.167	−0.64	57.175
74	56	−0.029	4.39	46.420
76	7	0.487	−3.983	53.913
76	28	0.071	4.074	50.719
76	56	−0.224	10.7	33.099
78	7	0.451	−2.433	63.989
78	28	0.286	1.192	95.932
78	56	0.217	5.05	85.568
80	7	1.132	−9.027	87.012
80	28	0.491	3.923	90.053
80	56	−0.031	16.267	52.724

and from 0.56 to 4.52 MPa for 56 days. For CUTB samples with a solid content of 78 wt.%, these rates increased from 0.58 to 3.84 MPa for 7 days, from 0.73 to 6.58 MPa for 28 days, and from 0.82 to 6.83 MPa for 56 days. The compressive strength of the CUTB samples with the high c/t ratio increases faster with the curing time because the cement can produce a large amount of C-S-H and ettringite with strong gelling properties during the hydration reaction. The hydration product increases the degree of internal compaction and increases the strength of the CUTB samples.

The solid content and curing time values were considered as constants to better study the UCS variation of CUTB samples with different cement-to-tailings ratios. The relationship between the CUTB's strength and c/t ratio shows quadratic properties, and the relevant correlation coefficients (R^2) were listed in Table 16.

It was found from Table 16 that quadratic function regression has high fitting degrees whose responding multiple R^2 are larger than 0.95. Moreover, it was also found experimentally that the UCS performance of CUTB samples increases with increasing cement-to-tailings ratio, and when the curing time is 7 days and the c/t ratio is lower than 1 : 12, the regression model reflects that the strength of the CUTB increases slowly with the increase of the c/t ratio. The relationship between c/t ratio and UCS of CUTB samples could be well expressed as the quadratic equation, and the relevant expression can be defined as

$$\mathrm{UCS} = A_2 + B_2 \times (\mathrm{c/t}) + C_1 (\mathrm{c/t})^2, \quad (8)$$

where c/t is the cement-to-tailings ratio; A_2, B_2, and C_1 are the fitting parameters related to the influence of c/t and UCS factors. The equation parameters were listed in Table 17.

3.2.4. Effect of Curing Time. Dotted-line graphs of the backfill's strength of different curing time and c/t ratio are shown in Figure 9. Since the curing time is only 7, 28, and 56 days, the three-point data do not draw a trend line, so no relevant data fitting analysis has been conducted. Instead, one can observe from results that as curing time increases, the compressive strength performance of CUTB samples increases.

For instance, the strengths of CUTB with a cement-to-tailings ratio of 1 : 04 and solid content of 80 wt.% are 4.32, 7.11, and 7.34 MPa for curing times of 7, 28, and 56 days, respectively. At a fixed cement-to-tailings (1 : 04), these values were 2.13, 2.84, and 3.11 MPa; 2.45, 3.58, and 3.97 MPa; 2.86, 4.26, and 4.52 MPa; and 3.84, 6.58, and 6.83 MPa for a solid content of 72%, 74%, 76%, and 78%, respectively. As expected, for a given c/t ratio and curing time, the higher the solid content, the higher the increase rate of the backfill's strength. In addition, when the curing time is larger than 28 days, the backfill's strength increases slowly.

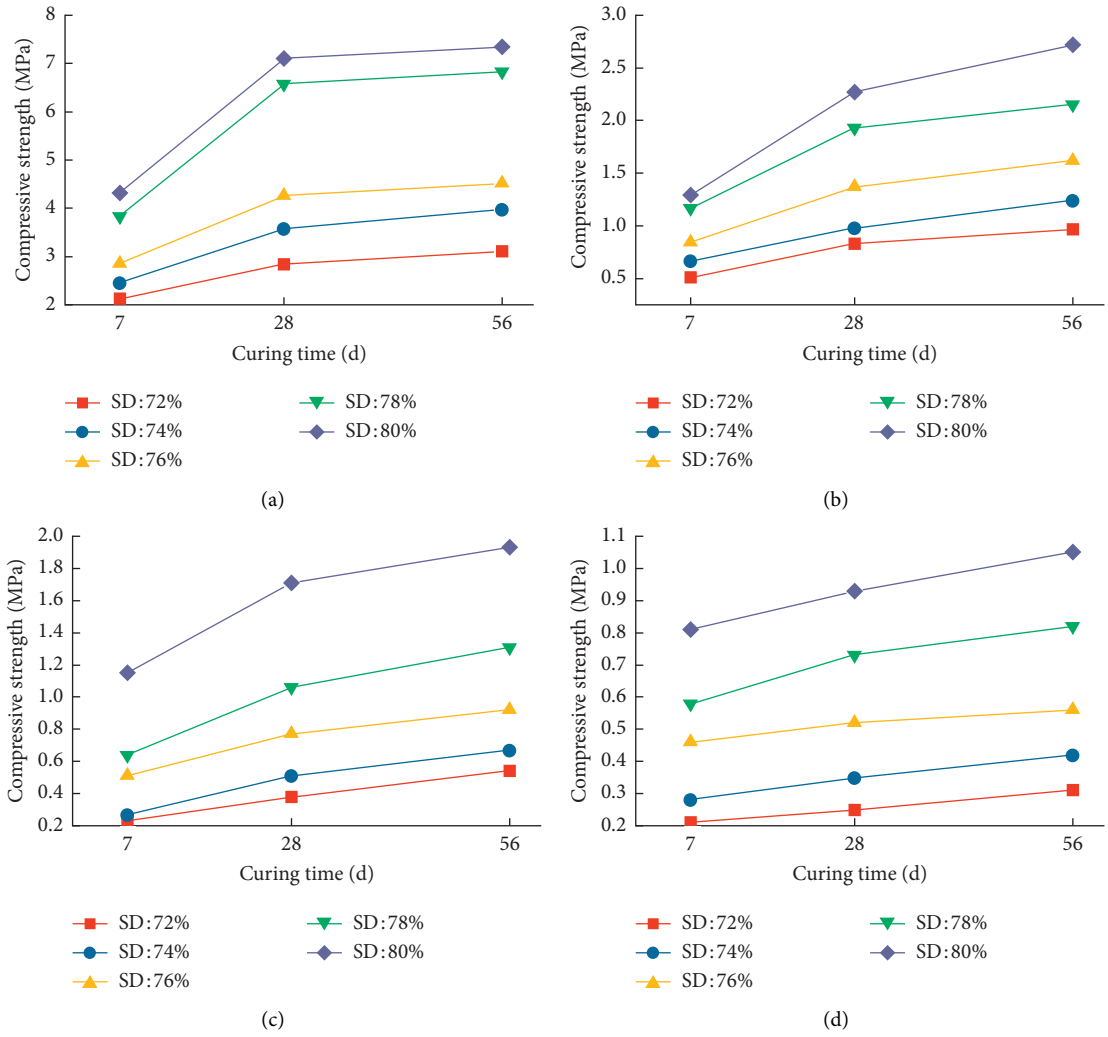

Figure 9: Relationship between CT and UCS of CUTB: (a) c/t: 1 : 04; (b) c/t: 1 : 08; (c) c/t: 1 : 12; (d) c/t: 1 : 16.

3.2.5. Prediction Model of CUTB's Compressive Strength. In order to establish the prediction model of CUTB's compressive strength under the change of cement-to-tailings ratio and solid content at different curing times, nonlinear regression analysis was used and relevant expressions at different curing times (7 d, 28 d, and 56 d) can be defined in equations (9), (10), and (11), respectively.

$$\mathrm{UCS}_{7\mathrm{d}} = 53.7 - 1.4\mathrm{SD} - 89.5\,(\mathrm{c/t}) + 58.4\,(\mathrm{c/t})^2 + 1.1\mathrm{SD}\,(\mathrm{c/t}), \tag{9}$$

$$\mathrm{UCS}_{28\mathrm{d}} = 85.85 - 2.2\mathrm{SD} - 194.3\,(\mathrm{c/t}) + 66.1\,(\mathrm{c/t})^2 + 2.6\mathrm{SD}\,(\mathrm{c/t}), \tag{10}$$

$$\mathrm{UCS}_{56\mathrm{d}} = 89.2 - 2.3\mathrm{SD} - 179.7\,(\mathrm{c/t}) + 50.5\,(\mathrm{c/t})^2 + 2.5\mathrm{SD}\,(\mathrm{c/t}), \tag{11}$$

where c/t is the cement-to-tailings ratio and SD is the solid content.

In the above prediction model, the multiple R^2 of equations (9)–(11) are 0.993, 0.988, and 0.990, respectively. Therefore, these models can well predict the variation of CUTB's compressive strength under the change of cement-to-tailings ratio and solid content at different curing times.

4. Conclusions

Based on the results, the following conclusions can be drawn:

(1) CUTB samples exhibit shear thinning characteristics irrespective of cement-to-tailings ratio and solid content. The rheological process of the CUTB slurry is the result of multiple rheological model composites and the rheological properties can be the characterizations to distinguish the high concentration slurry mixes and low concentration slurry mixes.

(2) The effects of the c/t and SD on the rheological properties of CUTB slurry are investigated. The yield stress and viscosity of CUTB slurry increase with the

increase of SD and c/t and the relationship between two rheological property parameters and two factors can be expressed as the quadratic equation.

(3) The sensitivity of rheological properties to SD is strong, and the sensitivity is weak to c/t. The yield stress and mean viscosity of CUTB slurry with a solid content of 78 wt.% are significantly larger than the slurry with a solid content of 76 wt.%, which is 2 to 3 times larger. These results show that the CUTB's flowability with solid content below 76 wt.% is better.

(4) When the other two factors are fixed, the UCS of CUTB increases exponentially with the increase of solid content, while it increases with the cement-to-tailings ratio as quadratic.

(5) The larger c/t CUTB, the more significant effect of the curing time on the CUTB's strength. When the c/t gets smaller, the CUTB's strength increases slowly with solid content increasing. When the curing time is larger than 28 d, the backfill's strength is not significantly affected by the c/t ratio and solid content, and the strength increases slowly.

Data Availability

The data used to support the findings of this study are included within the article.

Conflicts of Interest

The authors declare that there are no conflicts of interest in this paper.

Acknowledgments

This project was supported by the Key Technology and Scientific and Technological Projects for prevention and control of major accidents in work safety of the State Administration of work safety (hunan-0008-2016AQ).

References

[1] M. Benzaazoua, M. Fall, and T. Belem, "A contribution to understanding the hardening process of cemented pastefill," *Minerals Engineering*, vol. 17, no. 2, pp. 141–152, 2004.

[2] A. Kesimal, E. Yilmaz, and B. Ercikdi, "Evaluation of paste backfill mixtures consisting of sulphide-rich mill tailings and varying cement contents," *Cement and Concrete Research*, vol. 34, no. 10, pp. 1817–1822, 2004.

[3] C. Qi, A. Fourie, and Q. Chen, "Neural network and particle swarm optimization for predicting the unconfined compressive strength of cemented paste backfill," *Construction and Building Materials*, vol. 159, pp. 473–478, 2018.

[4] C. Hou, W. Zhu, B. Yan, K. Guan, and J. Du, "Influence of binder content on temperature and internal strain evolution of early age cemented tailings backfill," *Construction and Building Materials*, vol. 189, pp. 585–593, 2018.

[5] J. Haiqiang, M. Fall, and L. Cui, "Yield stress of cemented paste backfill in sub-zero environments: experimental results," *Minerals Engineering*, vol. 92, pp. 141–150, 2016.

[6] L. Yang, J. Qiu, H. Jiang, S. Hu, H. Li, and S. Li, "Use of cemented super-fine unclassified tailings backfill for control of subsidence," *Minerals*, vol. 7, no. 11, p. 216, 2017.

[7] D. Wu, M. Fall, and S. J. Cai, "Coupling temperature, cement hydration and rheological behaviour of fresh cemented paste backfill," *Minerals Engineering*, vol. 42, pp. 76–87, 2013.

[8] E. Yilmaz, "Stope depth effect on field behaviour and performance of cemented paste backfills," *International Journal of Mining, Reclamation and Environment*, vol. 32, no. 4, pp. 273–296, 2018.

[9] W. U. Ai-Xiang, Y. Yang, H. Y. Cheng, S. M. Chen, and Y. Han, "Status and prospects of paste technology in China," *Chinese Journal of Engineering*, vol. 40, no. 5, pp. 517–525, 2018.

[10] P. Li, Y.-b. Hou, and M.-f. Cai, "Factors influencing the pumpability of unclassified tailings slurry and its interval division," *International Journal of Minerals, Metallurgy, and Materials*, vol. 26, no. 4, pp. 417–429, 2019.

[11] X. Deng, J. Zhang, B. Klein, N. Zhou, and B. de Wit, "Experimental characterization of the influence of solid components on the rheological and mechanical properties of cemented paste backfill," *International Journal of Mineral Processing*, vol. 168, pp. 116–125, 2017.

[12] X. Deng, B. Klein, L. Tong, and B. de Wit, "Experimental study on the rheological behavior of ultra-fine cemented backfill," *Construction and Building Materials*, vol. 158, pp. 985–994, 2018.

[13] Y. Wang, A. Wu, L. Zhang, F. Jin, and X. Liu, "Investigating the effect of solid components on yield stress for cemented paste backfill via uniform design," *Advances in Materials Science and Engineering*, vol. 2018, pp. 1–7, 2018.

[14] R. Alyousef, O. Benjeddou, C. Soussi, M. A. Khadimallah, and M. Jedidi, "Experimental study of new insulation lightweight concrete block floor based on perlite aggregate, natural sand, and sand obtained from marble waste," *Advances in Materials Science and Engineering*, vol. 2019, pp. 1–14, 2019.

[15] S. Panchal, D. Deb, and T. Sreenivas, "Variability in rheology of cemented paste backfill with hydration age, binder and superplasticizer dosages," *Advanced Powder Technology*, vol. 29, no. 9, pp. 2211–2220, 2018.

[16] L. Huynh, D. A. Beattie, D. Fornasiero, and J. Ralston, "Effect of polyphosphate and naphthalene sulfonate formaldehyde condensate on the rheological properties of dewatered tailings and cemented paste backfill," *Minerals Engineering*, vol. 19, no. 1, pp. 28–36, 2006.

[17] D. Simon and M. Grabinsky, "Apparent yield stress measurement in cemented paste backfill," *International Journal of Mining, Reclamation and Environment*, vol. 27, no. 4, pp. 231–256, 2013.

[18] X. J. Deng, B. Klein, D. J. Hallbom, B. de Wit, and J. X. Zhang, "Influence of particle size on the basic and time-dependent rheological behaviors of cemented paste backfill," *Journal of Materials Engineering and Performance*, vol. 27, no. 7, pp. 3478–3487, 2018.

[19] M. Fall, M. Benzaazoua, and E. G. Saa, "Mix proportioning of underground cemented tailings backfill," *Tunnelling and Underground Space Technology*, vol. 23, no. 1, pp. 80–90, 2008.

[20] B. Ercikdi, H. Baki, and M. İzki, "Effect of desliming of sulphide-rich mill tailings on the long-term strength of cemented paste backfill," *Journal of Environmental Management*, vol. 115, pp. 5–13, 2013.

[21] F. Cihangir, B. Ercikdi, A. Kesimal, A. Turan, and H. Deveci, "Utilisation of alkali-activated blast furnace slag in paste backfill of high-sulphide mill tailings: effect of binder type and dosage," *Minerals Engineering*, vol. 30, pp. 33–43, 2012.

[22] B. Koohestani, T. Belem, A. Koubaa, and B. Bussière, "Experimental investigation into the compressive strength development of cemented paste backfill containing nano-silica," *Cement and Concrete Composites*, vol. 72, pp. 180–189, 2016.

[23] A. Kesimal, E. Yilmaz, B. Ercikdi, I. Alp, and H. Deveci, "Effect of properties of tailings and binder on the short-and long-term strength and stability of cemented paste backfill," *Materials Letters*, vol. 59, no. 28, pp. 3703–3709, 2005.

[24] B. Ercikdi, A. Kesimal, F. Cihangir, H. Deveci, and İ. Alp, "Cemented paste backfill of sulphide-rich tailings: importance of binder type and dosage," *Cement and Concrete Composites*, vol. 31, no. 4, pp. 268–274, 2009.

[25] S. Yin, A. Wu, K. Hu, Y. Wang, and Y. Zhang, "The effect of solid components on the rheological and mechanical properties of cemented paste backfill," *Minerals Engineering*, vol. 35, pp. 61–66, 2012.

[26] B. Ercikdi, T. Yilmaz, and G. Külekci, "Strength and ultrasonic properties of cemented paste backfill," *Ultrasonics*, vol. 54, no. 1, pp. 195–204, 2014.

[27] W. Li and M. Fall, "Sulphate effect on the early age strength and self-desiccation of cemented paste backfill," *Construction and Building Materials*, vol. 106, pp. 296–304, 2016.

[28] B. Koohestani, A. Koubaa, T. Belem, B. Bussière, and H. Bouzahzah, "Experimental investigation of mechanical and microstructural properties of cemented paste backfill containing maple-wood filler," *Construction and Building Materials*, vol. 121, pp. 222–228, 2016.

[29] J. Zheng, Y. Zhu, and Z. Zhao, "Utilization of limestone powder and water-reducing admixture in cemented paste backfill of coarse copper mine tailings," *Construction and Building Materials*, vol. 124, pp. 31–36, 2016.

[30] J. Qiu, L. Yang, X. Sun, J. Xing, and S. Li, "Strength characteristics and failure mechanism of cemented super-fine unclassified tailings backfill," *Minerals*, vol. 7, no. 4, p. 58, 2017.

[31] Q.-s. Chen, Q.-l. Zhang, A. Fourie, X. Chen, and C.-c. Qi, "Experimental investigation on the strength characteristics of cement paste backfill in a similar stope model and its mechanism," *Construction and Building Materials*, vol. 154, pp. 34–43, 2017.

[32] S. Cao, E. Yilmaz, and W. Song, "Evaluation of viscosity, strength and microstructural properties of cemented tailings backfill," *Minerals*, vol. 8, no. 8, p. 352, 2018.

[33] C. Qi, A. Fourie, Q. Chen, and P. Liu, "Application of first-principles theory in ferrite phases of cemented paste backfill," *Minerals Engineering*, vol. 133, pp. 47–51, 2019.

[34] Y. He, Q. Chen, C. Qi, Q. Zhang, and C. Xiao, "Lithium slag and fly ash-based binder for cemented fine tailings backfill," *Journal of Environmental Management*, vol. 248, Article ID 109282, 2019.

[35] Q. Chen, Q. Zhang, C. Qi, A. Fourie, and C. Xiao, "Recycling phosphogypsum and construction demolition waste for cemented paste backfill and its environmental impact," *Journal of Cleaner Production*, vol. 186, pp. 418–429, 2018.

[36] Q. Chen, Q. Zhang, A. Fourie, and C. Xin, "Utilization of phosphogypsum and phosphate tailings for cemented paste backfill," *Journal of Environmental Management*, vol. 201, pp. 19–27, 2017.

[37] X. Xue, Y. Ke, Q. Kang et al., "Cost-effective treatment of hemihydrate phosphogypsum and phosphorous slag as cemented paste backfill material for underground mine," *Advances in Materials Science and Engineering*, Article ID 9087538, 11 pages, 2019.

[38] M. L. Walske, H. McWilliam, J. Doherty, and A. Fourie, "Influence of curing temperature and stress conditions on mechanical properties of cementing paste backfill," *Canadian Geotechnical Journal*, vol. 53, no. 1, pp. 148–161, 2015.

[39] C. Qi, Q. Chen, A. Fourie, and Q. Zhang, "An intelligent modelling framework for mechanical properties of cemented paste backfill," *Minerals Engineering*, vol. 123, pp. 16–27, 2018.

[40] S. Cao, W. Song, and E. Yilmaz, "Influence of structural factors on uniaxial compressive strength of cemented tailings backfill," *Construction and Building Materials*, vol. 174, pp. 190–201, 2018.

[41] S. Cao and W. Song, "Effect of filling interval time on the mechanical strength and ultrasonic properties of cemented coarse tailing backfill," *International Journal of Mineral Processing*, vol. 166, pp. 62–68, 2017.

[42] S. Cao, W.-D. Song, G.-L. Xue, Y. Wang, and P.-R. Zhu, "Tests of strength reduction of cemented tailings filling considering layering character," *Rock and Soil Mechanics*, vol. 36, no. 10, pp. 2869–2876, 2015.

[43] W. Song, J. Wang, Y. Tan, and S. Cao, "Energy consumption and damage characteristics of stratified backfill under triaxial loading and unloading," *Journal of China University of Mining and Technology*, vol. 46, no. 5, pp. 1050–1056, 2017.

[44] J. Wang, W. Song, S. Cao, and Y. Tan, "Mechanical properties and failure modes of stratified backfill under triaxial cyclic loading and unloading," *International Journal of Mining Science and Technology*, vol. 28, 2018.

[45] ASTM International, *Standard Test Method for Compressive Strength of Cylindrical Concrete Specimens*, ASTM International, West Conshohocken, PA, USA, ASTM C39/C39M-12a, 2012.

[46] B. Alejo and A. Barrientos, "Model for yield stress of quartz pulps and copper tailings," *International Journal of Mineral Processing*, vol. 93, no. 3-4, pp. 213–219, 2009.

[47] Z. Ding, Z. Yin, L. Liu, and Q. Chen, "Effect of grinding parameters on the rheology of pyrite-heptane slurry in a laboratory stirred media mill," *Minerals Engineering*, vol. 20, no. 7, pp. 701–709, 2007.